


ORIGINAL ARTICLE

Open Access



Chemical constituents from the medicinal herb-derived fungus *Chaetomium globosum* Km1226

Chia-Hao Chang¹, George Hsiao^{2,3}, Shih-Wei Wang^{4,5,6,7}, Juei-Yu Yen^{5,8}, Shu-Jung Huang¹, Wei-Chiung Chi^{9*} and Tzong-Huei Lee^{1*} 

Abstract

Background Endophytic fungi have proven to be a rich source of novel natural products with a wide-array of biological activities and higher levels of structural diversity.

Results Chemical investigation on the liquid- and solid-state fermented products of *Chaetomium globosum* Km1226 isolated from the littoral medicinal herb *Atriplex maximowicziana* Makino resulted in the isolation of compounds **1–14**. Their structures were determined by spectroscopic analysis as three previously undescribed C₁₃-polyketides, namely aureonitol C (**1**), mollipilins G (**2**), and H (**3**), along with eleven known compounds **4–14**. Among these, mollipilin A (**5**) exhibited significant nitric oxide production inhibitory activity in LPS-induced BV-2 microglial cells with an IC₅₀ value of 0.7 ± 0.1 μM, and chaetoglobosin D (**10**) displayed potent anti-angiogenesis property in human endothelial progenitor cells (EPCs) with an IC₅₀ value of 0.8 ± 0.3 μM.

Conclusions Three previously unreported compounds **1–3** were isolated and identified. Mollipilin A (**5**) and chaetoglobosin D (**10**) could possibly be developed as anti-inflammatory and anti-angiogenic lead drugs, respectively.

Keywords *Chaetomium globosum*, Aureonitol, Mollipilin, Polyketide, Anti-inflammation, Anti-angiogenesis

*Correspondence:

Wei-Chiung Chi
joan@nqu.edu.tw
Tzong-Huei Lee
thlee1@ntu.edu.tw

¹Institute of Fisheries Science, College of Life Science, National Taiwan University, Taipei 10617, Taiwan

²Department of Pharmacology, School of Medicine, College of Medicine, Taipei Medical University, Taipei 11031, Taiwan

³Graduate Institute of Medical Sciences, College of Medicine, Taipei Medical University, Taipei 11031, Taiwan

⁴Department of Medicine, MacKay Medical College, New Taipei City 25245, Taiwan

⁵Institute of Biomedical Sciences, Mackay Medical College, New Taipei City 25245, Taiwan

⁶School of Pharmacy, College of Pharmacy, Kaohsiung 807378, Taiwan

⁷Department of Chinese Medicine, MacKay Memorial Hospital, Taipei 10449, Taiwan

⁸Department of Chinese Medicine, MacKay Memorial Hospital, Taipei 10491, Taiwan

⁹Department of Food Science, National Quemoy University, Kinmen 89250, Taiwan

Background

Endophytes are microorganisms that spend part or whole of their life cycles inside the healthy tissues of host plants, typically causing no apparent symptoms of diseases (Debbab et al. 2011; Kaul et al. 2012; Wang et al. 2017a; Ancheeva et al. 2020). In the symbiotic relationship, the endophytes are fed and protected by the host plants, and in return, the microorganisms produce bioactive secondary metabolites involving in the growth of the host plant and protecting the plants from pathogens and herbivores (Abdel-Azeem et al. 2016; Yang et al. 2021; Zhang et al. 2021; Collinge et al. 2022). The fungi, one major category of the endophytes, have been reported to be capable of producing a diverse array of specialized metabolites, and can produce chemical entities that are also present in plants or have similar biological activities as the compounds from plant sources (Mishra et al. 2022; Wen et al. 2022). Therefore, natural products derived from endophytic fungi were considered to be indispensable sources of new drugs with particular significance in lead structure discovery, due to their wide structural diversity and biological activities (Kumar et al. 2019; Qi et al. 2020; Song et al. 2020; Hridoy et al. 2022; Tiwari et al. 2022).

The medicinal herb *Atriplex maximowicziana* Makino (Chenopodiaceae), also known as Hae-Fwu-Rong, distributed widely at sandy and coral-rocky seashores of East Asia, and the whole plant has long been used in folk remedies for dispelling pathogenic wind and treating rheumatoid arthritis (Chang et al. 2022). Since the production scale of this herb was not sufficient for commercialization, its associated microorganisms could possibly be an alternative source of the effective specialized compounds. In this study, the fungal strain *Chaetomium globosum* Km1226 (Chaetomiaceae) was isolated from the leaves of *A. maximowicziana* Makino. *C. globosum* Km1226 cultured in PDY media furnished the crude extracts that exhibited significant antimicrobial activity at a concentration of 1.0 mg/mL in a preliminary biological evaluation. These results prompted the isolation and identification of fourteen constituents including seven C₁₃-polyketides including aureonitol C (1), mollipilins H and G (2 and 3), (-)-aureonitol (4), mollipilins A, E, and F (5–7), together with five cytochalasan alkaloids, chaetoglobosins A (8), C (9), and D (10), and aureochaetoglobosins B (11) and C (12), and two azaphilones, chaetoviridin A (13), and chaetomugilin A (14) (Fig. 1). Herein, the isolation and structural characterization of previously unreported compounds were discussed along with their nitric oxide production inhibitory and anti-angiogenic activities.

Results

The EtOAc extract of fermented broths of *C. globosum* Km1226 was fractionated and purified sequentially by column chromatography on Sephadex LH-20 and

semipreparative HPLC to yield undescribed compounds 1–3 as well as eleven known compounds 4–14.

Compound 1 was obtained as white powder, and was deduced to have the molecular formula C₁₃H₁₈O₃ as evidenced from a quasi-molecular ion [M+H]⁺ at *m/z* 223.1329 (calcd 223.1334 for C₁₃H₁₉O₃) in the HRESIMS, supported by analysis of ¹³C NMR data (Table 1), indicating 5 degrees of unsaturation. Its IR spectrum displayed absorptions at 3357 cm⁻¹, indicating the presence of a hydroxy group. Analysis of ¹H NMR and HSQC spectra of 1 indicated signals for six mutually *trans*-coupled olefinic protons at δ_H 6.31 (1H, dd, *J*=15.0, 10.2 Hz, H-3), 5.72 (1H, dd, *J*=15.0, 7.2 Hz, H-4), 5.61 (1H, dd, *J*=14.4, 7.8 Hz, H-8), 6.20 (1H, dd, *J*=14.4, 10.2 Hz, H-9), 6.23 (1H, ddt, *J*=15.0, 10.2, 1.2 Hz, H-10), and 5.76 (1H, dt, *J*=15.0, 5.4 Hz, H-11), two mutually coupled carbinoyl methines at δ_H 4.06 (1H, m, H-5) and 3.70 (1H, t, *J*=7.8 Hz, H-6), two oxygenated methylenes at δ_H 4.08 (2H, dd, *J*=5.4, 1.2 Hz, H-12) and 4.06 (1H, m, H_a-13) and 3.70 (1H, t, *J*=7.8 Hz, H_b-13), one exomethylene at δ_H 5.22 (1H, dd, *J*=16.2, 1.8 Hz, H_a-1) and 5.09 (1H, dd, *J*=10.2, 1.8 Hz, H_b-1), one olefinic proton at δ_H 6.36 (1H, dt, *J*=16.2, 10.2 Hz, H-2), and one methine at δ_H 2.83 (1H, quintet, *J*=7.8 Hz, H-7) (Table 2). Interpretation of the ¹³C NMR accompanied by HSQC spectra revealed 13 carbon signals attributable to seven olefinic methines at δ_C 131.8 (C-10), 132.9 (C-8), 133.0 (C-11), 133.3 (C-4), 133.4 (C-9), 134.2 (C-3), and 137.8 (C-2), three methylenes at δ_C 63.4 (C-12), 72.1 (C-13), and 118.2 (C-1), and three aliphatic methines at δ_C 52.6 (C-7), 82.6 (C-6), and 86.5 (C-5). Several distinctive signals at δ_C 63.4 (C-12), 72.1 (C-13), 82.6 (C-6) and 86.5 (C-5) were assigned to oxygen-bearing carbons. Cross-peaks of H-1/H-2, H-2/H-3, H-3/H-4, H-4/H-5, H-5/H-6, H-6/H-7, H-7/H-8, H-8/H-9, H-9/H-10, H-10/H-11, H-11/H-12, and H-7/H-13 in the COSY spectrum together with key cross-peaks of H-3/C-5, H-4/C-6, H-8/C-6, H-9/C-7, H-8/C-13, and H-13/C-5 in the HMBC spectrum (Fig. 2) established the plain structure of 1 as shown. The NOESY correlation of H-5/H-7 (Fig. 2), *J* values (7.8 Hz) of mutually coupled H-7/H-6 and H-6/H-5, and no NOESY correlation of H-7/H-6 and H-6/H-5 established the relative configurations of H-5, H-6, and H-7 to be *S*^{*}, *R*^{*}, and *S*^{*}, respectively. The plain structure of 1 was almost compatible with that of (-)-aureonitol (4) except that a terminal CH₃-12 in 4 was substituted by a hydroxymethyl in 1. The absolute configuration of 1 of the chiral carbons in the tetrahydrofuran moiety determined as 5*S*, 6*R*, and 7*S* was found to be the same with those of 4 as evidenced from the positive Cotton effect at 220–250 nm in the CD spectra of both 1 and 4 (Fig. S10) and sign of the optical rotational values of 1 ([α]_D²⁷ -9.8) and 4 ([α]_D²⁵ -31.3) in the literature (Nakazawa et al. 2013).

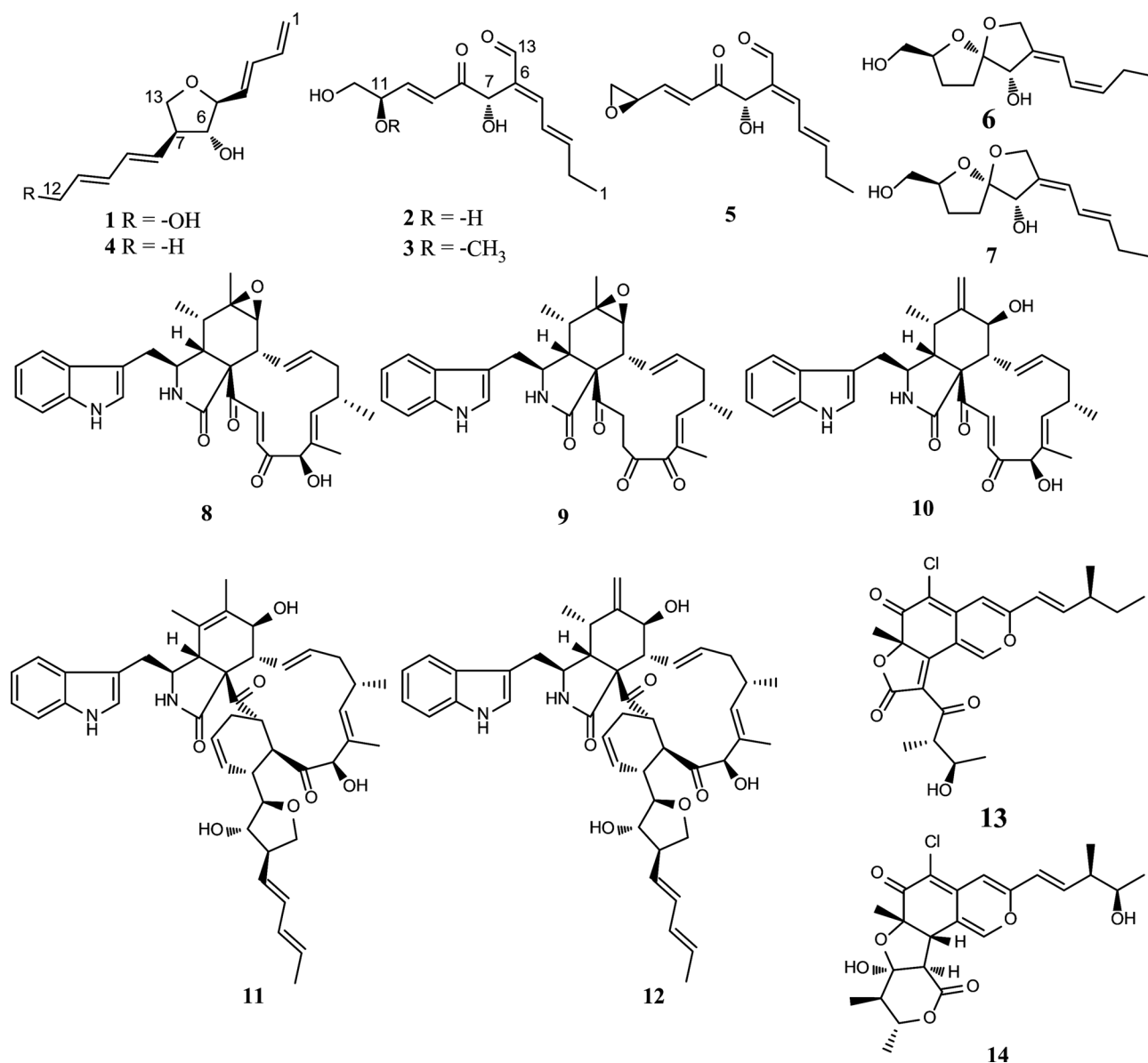


Fig. 1 Chemical structures of compounds 1–14 identified in this study

The HRESIMS of compound 2 showed a quasi-molecular ion peak at m/z 255.1227 $[M+H]^+$ (calcd 255.1232 for $C_{13}H_{19}O_5$) and a deprotonated molecular ion $[M-H]^-$ at m/z 253.1087 (calcd 253.1081 for $C_{13}H_{17}O_5$), supported by analysis of ^{13}C NMR data (Table 1), indicating 5 degrees of unsaturation. Its IR spectrum displayed absorptions at 3365, 1704, and 1672 cm^{-1} , indicating the presence of a hydroxy, an α,β -unsaturated aldehyde, and an α,β -unsaturated ketone, respectively. The 1H NMR spectrum of 2 showed signals for five mutually-coupled olefinic protons at δ_H 6.50 (1H, dt, $J=15.0, 6.6$ Hz, H-3), 6.76 (1H, ddt, $J=15.0, 12.0, 1.2$ Hz, H-4), 7.20 (1H, d, $J=12.0$ Hz, H-5), and 6.41 (1H, dd, $J=15.6, 1.8$ Hz, H-9), and 6.98 (1H, ddd, $J=15.6, 5.0, 1.8$ Hz, H-10), two carbinoyl methines at δ_H 5.43 (1H, s, H-7) and 4.25 (1H, br

q, $J=5.0$ Hz, H-11), one aldehydic methine at δ_H 9.42 (1H, s, H-13), one oxymethylene at δ_H 3.51 (1H, dd, $J=10.8, 5.0$ Hz, H_a-12) and 3.48 (1H, dd, $J=10.8, 5.0$ Hz, H_b-12), one methylene at δ_H 2.29 (2H, qd, $J=7.2, 6.6$ Hz, H-2), and one methyl at δ_H 1.09 (3H, t, $J=7.2$, H-1) (Table 2), which were supported by the COSY assignments of 2. Interpretation of the ^{13}C NMR accompanied by HSQC spectrum revealed 13 carbon signals attributable to seven olefinic methines at δ_C 125.6 (C-9), 126.4 (C-4), 148.5 (C-10), 153.3 (C-3), 155.9 (C-5), and 194.9 (C-13), two aliphatic methylenes at δ_C 27.7 (C-2) and 66.5 (C-12), two nonprotonated carbons at δ_C 137.4 (C-6) and 199.1 (C-8), two aliphatic methines at δ_C 71.5 (C-7) and 73.1 (C-11), and one methyl at δ_C 13.2 (C-1). Of all the assigned carbon signals, three distinctive signals at δ_C 66.5 (C-12),

Table 1 ^{13}C NMR spectroscopic data for compounds **1–3** (δ in ppm)

	1^a	2^a	3^a
position	δ_{C} , mult	δ_{C} , mult	δ_{C} , mult
1	118.2 d	13.2 q	13.2 q
2	137.8 d	27.7 t	27.7 t
3	134.2 d	153.3 d	153.4 d
4	133.3 d	126.4 d	126.4 d
5	86.5 d	155.9 d	155.9 d
6	82.6 d	137.4 s	137.5 s
7	52.6 d	71.5 d	71.5 d
8	132.9 d	199.1 s	198.9 s
9	133.4 d	125.6 d	127.5 d
10	131.8 d	148.5 d	145.6 d
11	133.0 d	73.1 d	83.1 d
12	63.4 t	66.5 t	64.8 t
13	72.1 t	194.9 d	194.9 d
11-OCH ₃			57.9 q

^aMeasured in methanol-*d*₄ (150 MHz)

71.5 (C-7), and 73.1 (C-11) were assigned to be oxygenated carbons. Key cross-peaks of H-5, -7, and -13/C-6, H-5 and -13/C-7, H-5 and -7/C-13, and H-7, -9, and -10/C-8 in the HMBC spectrum (Fig. 1) indicated the gross structure of **2** was as shown. The configurations of Δ^3 , Δ^5 , and Δ^9 were deduced to be all *E* forms based on a coupling constant of H-3/H-4 ($J=15.0$ Hz), a key NOESY correlation of H-5/H-13 (Fig. 2), and a coupling constant of H-9/H-10 ($J=15.6$ Hz), respectively. Due to biogenetic relationship, the relative configuration of C-7 and -11 in

2 was speculated to be the same with those of mollipilin A (**5**). The experimental CD spectrum of **2** was compatible with that of **5** (Fig. S28), and the sign of optical rotational value of **2** ($[\alpha]_{\text{D}}^{27}+22.2$) was the same with that of **5** ($[\alpha]_{\text{D}}^{25}+39.3$) in the literature (Asai et al. 2012). The absolute configurations of C-7 and -11 of **2** were deduced to be *S* and *R*, respectively, as shown in Fig. 1.

The HRESIMS of compound **3** showed protonated molecular ion peaks at m/z 269.1383 $[\text{M}+\text{H}]^+$ (calcd 269.1389 for $\text{C}_{14}\text{H}_{21}\text{O}_5$) and a deprotonated molecular ion $[\text{M}-\text{H}]^-$ at m/z 267.1242 (calcd 267.1238 for $\text{C}_{14}\text{H}_{19}\text{O}_5$), indicating a molecular formula of $\text{C}_{14}\text{H}_{20}\text{O}_5$ for **3**. When comparing the ^1H and ^{13}C NMR data of **3** with those of **2**, compound **3** almost coincided well with **2** except that the substituent at C-11 in **3** was changed to be a methoxy as judged from the chemical shift of C-11 (δ_{C} 73.1) in **2** shifted to δ_{C} 83.1 in **3**. A key cross-peak of -OCH₃/C-11 in the HMBC spectrum corroborated that the additional methoxy group was attached at C-11. The gross structure of **3** was thus determined. Since both the experimental CD spectrum of **3** (Fig. S28) and the sign of optical rotational value of **3** were in compliance with those of **2**, the absolute configuration of **3** was determined to be the same as that of **2**.

(-)-Aureonitol (**4**), a tetrahydrofuran derivative, has been isolated from *C. globosum*, and was found to act like a transcriptional regulator for the biosynthesis of other secondary metabolites in that fungal species (Nakazawa et al. 2013). The structure of mollipilin A (**5**), an epoxide-containing polyketide, was found to exhibit moderate

Table 2 ^1H NMR spectroscopic data for compounds **1–3** (δ in ppm, mult., J in Hz)

	1^a	2^a	3^a
position	δ_{H} , mult (J in Hz)	δ_{H} , mult (J in Hz)	δ_{H} , mult (J in Hz)
1a	5.22 dd (16.2, 1.8)	1.09 t (7.2)	1.10 t (7.2)
1b	5.09 dd (10.2, 1.8)		
2	6.36 dt (16.2, 10.2)	2.29 qd (7.2, 7.2) 2.29 qd (7.2, 7.2)	2.30 qd (7.2, 7.2) 2.30 qd (7.2, 7.2)
3	6.31 dd (15.0, 10.2)	6.50 dt (15.0, 7.2)	6.51 dt (15.0, 7.2)
4	5.72 dd (15.0, 7.2)	6.76 ddt (15.0, 12.0, 1.2)	6.78 ddt (15.0, 10.2, 1.2)
5	4.06 m	7.20 d (12.0)	7.22 d (10.2)
6	3.70 t (7.8)		
7	2.83 quintet (7.8)	5.43 s	5.44 s
8	5.61 dd (14.4, 7.8)		
9	6.20 dd (14.4, 10.2)	6.41 dd (15.6, 1.8)	6.38 dd (15.6, 1.2)
10	6.23 ddt (15.0, 10.2, 1.2)	6.98 ddd (15.6, 5.0, 1.8)	6.79 dd (15.6, 6.0)
11	5.76 dt (15.0, 5.4)	4.25 br q (5.0)	3.85 qd (6.0, 1.2)
12a	4.08 dd (5.4, 1.2)	3.51 dd (10.8, 5.0)	3.55 dd (10.2, 6.0)
12b		3.48 dd (10.8, 5.0)	3.49 dd (10.2, 6.0)
13a	4.06 ^b	9.42 s	9.42 s
13b	3.70 t (7.8)		
11-OCH ₃			3.31 s

^aMeasured in methanol-*d*₄ (600 MHz)^bSignal without multiplicity was overlapped, and was picked up from HSQC experiment

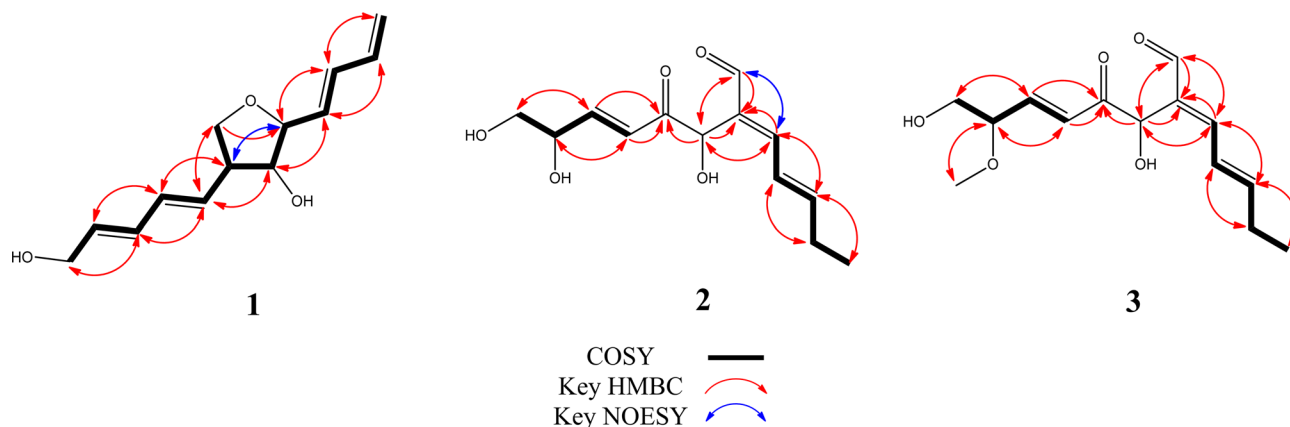


Fig. 2 COSY, key HMBC, and NOESY correlations of compounds 1–3

growth inhibitory effects on HCT-116 cells (Asai et al. 2012). Mollipilins E (6) and F (7), two *spiro*-furan-containing polyketides, accompanied with mollipilin A (5) have been isolated from *C. mollipilium* (Asai et al. 2012). Chaetoglobosins A, C, and D (8–10), three cytochalasan alkaloids, have been isolated from a *Ginkgo biloba*-derived fungal strain *C. globosum* No.04, and were found to exhibit potent anti-fungal effects (Zhang et al. 2019). Aureochaeglobosins B and C (11 and 12), two rare aureonitol derivative-fused chaetoglobosins via [4+2] cycloaddition, have been isolated from *C. globosum* (Yang et al. 2018). Chaetoviridin A (13) and chaetomugilin A (14), two chloro-azaphilones, have been found from *C. globosum* by using a molecular epigenetic approach (Wang et al. 2017), and showed significant cytotoxicity against cultured P388 cells and HL-60 cells (Yamada et al. 2008).

Compounds 1–14 were tested for anti-inflammatory and anti-angiogenic activities. The anti-inflammatory assay was performed by measuring the amount of nitric oxide (NO) production in lipopolysaccharide (LPS)-induced microglial BV-2 cells. Compounds 1–14 inhibited 42.3%, 50.2%, 51.7%, 68.2%, 111.6%, 44.7%, 48.2%, 92.6%, 71.8%, 45.7%, 99.1%, 90.6%, 72.9% and 45.0% of NO production (Fig. 3A), respectively, at a concentration of 20 μM without any cytotoxicity (Fig. 3B) except compounds 5 and 8. The positive control curcumin exhibited inhibition of NO production 100.4%. Of all the isolates, mollipilin A (5), aureochaeglobosins B (11) and C (12) exhibited significant nitric oxide production inhibitory activity in LPS-induced BV-2 microglial cells with IC_{50} values of 0.7 ± 0.1 , 1.2 ± 0.1 and 1.6 ± 0.2 μM , respectively (Table 3). Endothelial progenitor cells (EPCs) can dictate tumor angiogenesis and cancer progression by activating the angiogenic switch in tumor microenvironment. Therefore, targeting EPCs to develop anti-angiogenic agents is an attractive therapeutic approach for cancer treatment. In this study, it was found that compounds 5, 8, 9, 10, 11, and 12 showed promising growth-inhibitory

effects on EPCs with IC_{50} values ranging from 1 to 10 μM , with sorafenib as the positive control. As shown in Table 4, chaetoglobosin D (10) exhibited the most potent anti-angiogenic activity by suppressing EPCs growth ($\text{IC}_{50} = 0.8 \pm 0.3$ μM).

Conclusion

In summary, fourteen components 1–14, including three previously undescribed C_{13} -polyketides, aureonitol C (1), mollipilins G (2), and H (3), were identified from the cultures of endophytic *C. globosum* Km1226. Mollipilin A (5) and chaetoglobosin D (10) could be a potential agent for the development of anti-inflammatory and anti-angiogenic leads, respectively, and further studies are still needed to clarify the underlying mechanisms for the biological activities and the structure–activity relationship.

Methods

General experimental procedures

The optical rotations were measured on a JASCO P-2000 Digital Polarimeter (JASCO, Tokyo, Japan). The UV spectra were recorded on a Thermo UV-Visible Helios α Spectrophotometer (Thermo Scientific, Waltham, MA, USA). The IR spectra were obtained on a JASCO FT/IR 4100 spectrometer (Tokyo, Japan). The NMR spectra were recorded at 600 and 150 MHz for ^1H and ^{13}C , respectively, on an Agilent 600 MHz DD2 NMR spectrometer (Agilent, USA). HRESIMS spectra were determined on a Q Exactive Plus Hybrid Quadrupole-Orbitrap Mass Spectrometer (Thermo Fisher Scientific, Bremen, Germany). HPLC separation was performed on a Hitachi HPLC system coupled with a Bischoff RI-8120 RI Detector (Bischoff, Leonberg, Germany) and the Phenomenex Luna column (5 μm PFP column, 100 \AA , 250 \times 10.0 mm) (Torrance, CA, USA), SunFire column (5 μm C_{18} column, 100 \AA , 250 \times 10.0 mm) (Milford, Mass, USA) and Phenomenex Gemin column (5 μm C_{18} column, 110 \AA , 250 \times 4.6 mm) (Torrance, CA, USA). Open column

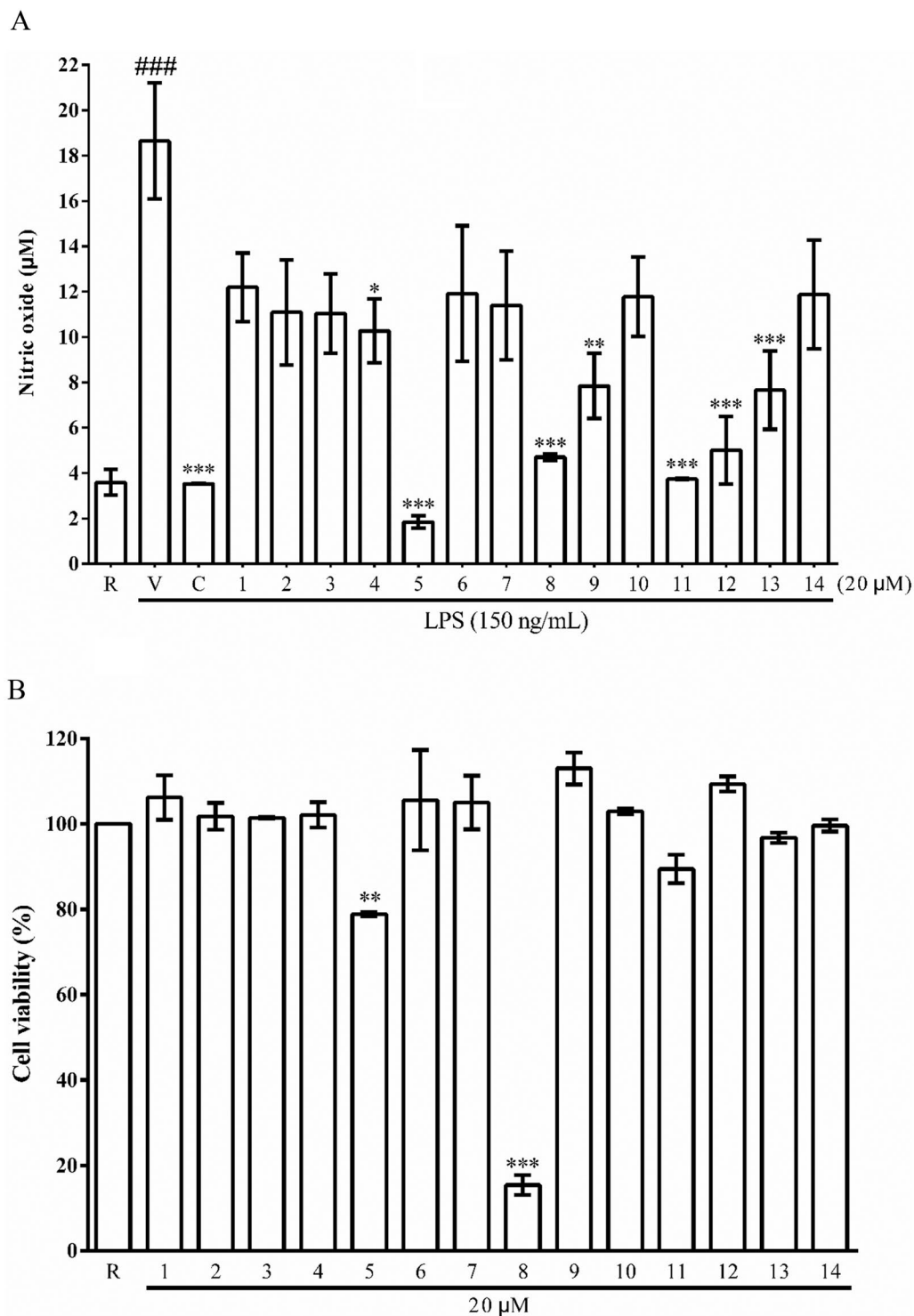


Fig. 3 Effects of compounds 1–14 on LPS-induced NO production in BV-2 cells (**A**) and their cytotoxicities (**B**). The concentration of test compounds was 20 µM (* $p < 0.05$, ** $p < 0.01$, and *** $p < 0.001$)

chromatography was performed with Sephadex LH-20 (Amersham Bioscience, Uppsala, Sweden). TLC was carried out with precoated silica gel 60 F254 (Merck, Darmstadt, Germany). Compounds were detected by UV and

10% aqueous H_2SO_4 spraying reagent followed by heating at 105 °C for 1 min. The solvents were analytical grade MeOH (Merck, Darmstadt, Germany) and ACN (Merck, Darmstadt, Germany) for HPLC.

Table 3 IC₅₀ values of **5**, **11**, and **12** on nitric oxide production inhibitory activities induced by lipopolysaccharide in microglial BV-2 cells

compound	IC ₅₀ (μM) ^{a,b}
5	0.7 ± 0.1***
11	1.2 ± 0.1**
12	1.6 ± 0.2**
Curcumin ^c	2.7 ± 0.3

p* < 0.01*p* < 0.001^aIC₅₀ = concentration that reduces NO production by 50%^bAsterisks denote significance compared to curcumin (positive control) according to the two-tailed *t*-test^cPositive control used in this study**Table 4** Anti-angiogenic activity of isolated compounds in human EPCs

compound	IC ₅₀ (μM) ^a
1	> 50
2	> 50
3	> 50
4	> 50
5	5.6 ± 0.1
6	> 50
7	> 50
8	4.6 ± 0.1
9	8.1 ± 0.4
10	0.8 ± 0.3
11	5.2 ± 0.3
12	2.9 ± 0.3
13	> 50
14	> 50
Sorafenib ^b	4.8 ± 0.3

^aEPCs were treated with the indicated compounds for 48 h. Anti-angiogenic effects were evaluated in a cell growth assay (*n* = 3). Data are displayed as the mean ± SEM^bPositive control used in this study

Fungal strain and culture

The fungal strain of *Chaetomium globosum* Km1226 was isolated from fresh leaf of *Atriplex maximowicziana* that were collected from Kinmen County, Republic of China, in May 2018. The fungus was identified according to morphological characteristics and the molecular biology method of amplifying the ITS gene sequence. The sequence data for this strain have been deposited in GenBank with the accession number OQ778818. The purified strain was cultivated in a CMA medium plate (Becton, Dickinson and Company, Sparks, MD, USA) at 29 °C for 14 days. Then agar were cut into small pieces (approximately 0.5 × 0.5 × 0.5 cm³) and inoculated into 144 × 250 mL flasks containing 100 mL of PDY medium (containing 10 g dextrose, 2 g peptone and 1 g yeast extract in 1 L distilled water) for liquid state fermentation and 15 × 250 mL flasks containing 10 mL of PDY medium and 20 g brown rice for solid state fermentation which were both

sterilized at 121 °C with high pressure. They were fermented for 14 days with shaker equipment at 180 rpm and 28 days at 26 °C, respectively.

Extraction and isolation of secondary metabolites

The fermentation broth (14.4 L) was filtered, the filtrate was extracted with EtOAc (2 × 14.4 L), and the resulting extract was evaporated under reduced pressure to afford a viscous solid (5.6 g), which was applied to Sephadex LH-20 column chromatography (2.5 cm i.d × 56 cm) and eluted with MeOH obtain eleven main fractions I–X based on TLC analyses. Fraction IV was further purified by semipreparative HPLC using Phenomenex Gemin C₁₈ column with 45% MeCN/H₂O containing 0.1% formic acid (1.0 mL/min) to obtain **1** (4.3 mg, *t_R* = 10.2 min), and SunFire C₁₈ column with 30% MeCN/H₂O containing 0.1% formic acid (2.0 mL/min) to obtain **2** (7.7 mg, *t_R* = 20.4 min) and **3** (9.6 mg, *t_R* = 18.5 min), and Phenomenex Luna PFP column with 80% MeCN/H₂O (2.0 mL/min) to obtain **4** (0.5 g, *t_R* = 11.6 min), and SunFire C₁₈ column with 30% MeCN/H₂O (2.0 mL/min) to obtain **5** (59.5 mg, *t_R* = 30.8 min), Phenomenex Luna PFP column with 65% MeOH/H₂O (2.0 mL/min) to obtain **6** (11.9 mg, *t_R* = 19.9 min) and **7** (5.2 mg, *t_R* = 22.1 min), Phenomenex Luna PFP column with 70% MeOH/H₂O (2.0 mL/min) to obtain **11** (6.4 mg, *t_R* = 53.6 min), **12** (12.6 mg, *t_R* = 39.0 min), **13** (16.3 mg, *t_R* = 13.8 min) and **14** (7.1 mg, *t_R* = 61.9 min).

The solid state fermented product (300 g) was lyophilized, ground into powder, and extracted with 1 L of MeOH three times. The combined methanolic extracts were evaporated into a brown residue (18.7 g), which was suspended in 500 mL of H₂O and partitioned with 500 mL of *n*-hexane three times for deoil, next partitioned with 500 mL of ethyl acetate three times then concentrated under vacuum to dryness (1.2 g). Subsequently, the ethyl acetate extract was redissolved in 10 mL of methanol and applied onto a Sephadex LH-20 column (2.5 cm i.d. × 56 cm) eluted with MeOH obtain eleven main fractions I–IV based on TLC analyses. Fraction III was further purified by semipreparative HPLC using Phenomenex Luna PFP column with 50% MeCN/H₂O containing 0.1% formic acid (2.0 mL/min) to obtain **8** (103.0 mg, *t_R* = 24.5 min), **9** (47.3 mg, *t_R* = 40.6 min) and **10** (5.2 mg, *t_R* = 13.3 min).

Aureonitol C (**1**): white powder; [α]_D²⁷ -9.8 (*c* 0.1, MeOH); UV (MeOH) λ_{max} (log ε) 232 (4.36), 272 (3.33) nm; IR (ATR) ν_{max} 3357, 2926, 2879, 1672, 1646, 1405, 1332, 1210, 1090, 1038 cm⁻¹; HRESIMS *m/z* 223.1329 [M+H]⁺ (calcd for C₁₃H₁₉O₃, 223.1334); ¹H NMR data (methanol-*d*₄, 600 MHz) see Table 2; ¹³C NMR data (methanol-*d*₄, 150 MHz) see Table 1.

Mollipilin G (**2**): yellowish amorphous; [α]_D²⁷ +22.2 (*c* 0.1, MeOH); UV (MeOH) λ_{max} (log ε) 230 (3.74), 280

(3.58) nm; IR (ATR) ν_{\max} 3365, 2940, 2841, 1704, 1672, 1634, 1452, 1395, 1267, 1198, 1112, 1019 cm^{-1} ; HRESIMS m/z 255.1227 $[\text{M}+\text{H}]^+$ (calcd for $\text{C}_{13}\text{H}_{19}\text{O}_5$, 255.1232) and 253.1087 $[\text{M}-\text{H}]^-$ (calcd for $\text{C}_{13}\text{H}_{17}\text{O}_5$, 253.1081); ^1H NMR data (methanol- d_4 , 600 MHz) see Table 2; ^{13}C NMR data (methanol- d_4 , 150 MHz) see Table 1.

Mollipilin H (3): yellowish amorphous; $[\alpha]_{\text{D}}^{27} +36.4$ (c 0.1, MeOH); UV (MeOH) λ_{\max} ($\log \epsilon$) 222 (3.65), 275 (3.39) nm; IR (ATR) ν_{\max} 3412, 2968, 2944, 2871, 2838, 1708, 1634, 1461, 1367, 1265, 1195, 1056, 1024 cm^{-1} ; HRESIMS m/z 269.1383 $[\text{M}+\text{H}]^+$ (calcd for $\text{C}_{14}\text{H}_{21}\text{O}_5$, 269.1389) and 267.1242 $[\text{M}-\text{H}]^-$ (calcd for $\text{C}_{14}\text{H}_{19}\text{O}_5$, 267.1238); ^1H NMR data (methanol- d_4 , 600 MHz) see Table 2; ^{13}C NMR data (methanol- d_4 , 150 MHz) see Table 1.

Cell culture

The mouse microglial BV-2 cell line was cultured as described previously (Lin et al. 2018). Before experiments, a confluence of 85% of cells were changed to 0.5% FBS media. Thereafter, cells were treated with vehicle or the indicated concentration of compounds 1–14 for 15 min and then stimulated with LPS (150 ng/mL) for 24 h. The conditioned medium was freshly collected and frozen at -80°C .

Inhibitory activity of nitric oxide (NO) production

Production of NO was evaluated by measuring the levels of nitrite in a conditioned medium as previously described with some modification (Hsieh et al. 2021). The culture supernatants were allowed to react with reconstituted cofactor solution and reconstituted nitrate reductase solution for 1 h at room temperature in the dark according to the instructions of the Nitrate/Nitrite Colorimetric Assay Kit (Cayman). Absorptions were measured at 550 nm using a microplate reader (MRX). Nitrite concentrations were calculated from the standard solutions of sodium nitrite. Curcumin was used as a positive control (Hsiao et al. 2020).

Cytotoxic activity

The cytotoxicity of compounds addressed in this study against the mouse microglial BV-2 cell line. The cell viability studies were determined by the MTT method. Cells were seeded in 24-well plates at 1×10^5 cells per well and grown for 24 h before use. The seeded cells were first treated with test compounds at 20 μM for 24 h. The final concentration of DMSO in the culture medium of the treated cells was adjusted to less than 0.5% (v/v) to prevent a solvent effect. DMSO was also treated as a vehicle control. Absorbance at 550 nm was obtained by a microplate reader (MRX). All of the experiments were performed in triplicate (Wu et al. 2022).

Anti-angiogenesis analysis

The methods employed for cell culture and cell growth assessments of human endothelial progenitor cells were conducted as previously reported (Lee et al. 2016; Yang et al. 2019).

Supplementary Information

The online version contains supplementary material available at <https://doi.org/10.1186/s40529-023-00406-8>.

Supplementary Materials 1: Figure S1. ^1H NMR (600 MHz, methanol- d_4) spectrum of compound 1. Figure S2. ^{13}C NMR (150 MHz, methanol- d_4) spectrum of compound 1. Figure S3. HSQC spectrum of compound 1. Figure S4. COSY spectrum of compound 1. Figure S5. HMBC spectrum of compound 1. Figure S6. NOESY spectrum of compound 1. Figure S7. IR (ZnSe) spectrum of compound 1. Figure S8. HRESIMS spectrum of compound 1. Figure S9. UV spectrum of compound 1 in MeOH. Figure S10. ECD spectra of compounds 1 and 4. Figure S11. ^1H NMR (600 MHz, methanol- d_4) spectrum of compound 2. Figure S12. ^{13}C NMR (150 MHz, methanol- d_4) spectrum of compound 2. Figure S13. HSQC spectrum of compound 2. Figure S14. COSY spectrum of compound 2. Figure S15. HMBC spectrum of compound 2. Figure S16. NOESY spectrum of compound 2. Figure S17. IR (ZnSe) spectrum of compound 2. Figure S18. HRESIMS spectrum of compound 2. Figure S19. UV spectrum of compound 2 in MeOH. Figure S20. ^1H NMR (600 MHz, methanol- d_4) spectrum of compound 3. Figure S21. ^{13}C NMR (150 MHz, methanol- d_4) spectrum of compound 3. Figure S22. HSQC spectrum of compound 3. Figure S23. COSY spectrum of compound 3. Figure S24. HMBC spectrum of compound 3. Figure S25. IR (ZnSe) spectrum of compound 3. Figure S26. HRESIMS spectrum of compound 3. Figure S27. UV spectrum of compound 3 in MeOH. Figure S28. ECD spectra of compounds 2, 3 and 5.

Acknowledgements

We thank Ms. A.G. in the Instrumentation Center of Taipei Medical University for the NMR data acquisition, respectively. This work was supported by a grant from the National Science and Technology Council (MOST 110-2320-B-002-023-MY3) of Taiwan to T.-H.L.

Author Contributions

C.-H.C. performed the experiments and drafted the initial manuscript. G.H. and S.-W.W. measured the biological activity data. T.-H.L. assisted with the supervision, methodology, and funding acquisition. W.-C.C. performed the conceptualization and data curation. All authors have read and approved the final manuscript.

Funding

This research was funded by the Ministry of Science and Technology of Taiwan for financial supports (MOST 110-2320-B-002-023-MY3) to T.-H.L.

Data Availability

Data of this study is available with the first author Mr. Chang.

Declarations

Ethics approval and consent to participate

Not applicable.

Consent for publication

Not applicable.

Competing interests

The authors declare that they have no known competing financial interests or personal relationships that could have influenced the work reported in this paper.

Received: 21 August 2023 / Accepted: 20 November 2023

Published online: 30 November 2023

References

- Abdel-Azeem MA, Zaki MS, Khalil FW, Makhlof AN, Farghaly ML (2016) Anti-rheumatoid activity of secondary metabolites produced by Endophytic *Chaetomium Globosum*. *Front Microbiol* 7:1477
- Ancheeva E, Daletos G, Proksch P (2020) Bioactive secondary metabolites from endophytic fungi. *Curr Med Chem* 27:1836–1854
- Asai T, Morita S, Shirata N, Taniguchi T, Monde K, Sakurai H, Ozeki T, Oshima Y (2012) Structural diversity of new C₁₃-polyketides produced by *Chaetomium mollipilium* cultivated in the presence of a NAD⁺-dependent histone deacetylase inhibitor. 14:5456–5459
- Chang CH, Lee YC, Hsiao G, Chang L-K, Chi WC, Cheng YC, Huang SJ, Wang TC, Lu YS, Lee TH (2022) Anti-epstein-barr viral agents from a medicinal herb-derived fungus *Alternaria Alstroemeriae* Km2286. *J Nat Prod* 85:2667–2674
- Collinge DB, Jensen B, Jørgensen HJ (2022) Fungal endophytes in plants and their relationship to plant Disease. *Curr Opin Microbiol* 69:102–177
- Debbab A, Aly HA, Prokseh P (2011) Bioactive secondary metabolites from endophytes and associated marine derived fungi. *Fungal Divers* 49:1–12
- Hriday M, Gorapi MZH, Noor S, Chowdhury NS, Rahman MM, Muscari I, Masia F, Adoriso S, Delfino DV, Mazid MA (2022) Putative anticancer compounds from Plant-Derived Endophytic Fungi A Review. *Molecules* 27:296
- Hsiao G, Wang SW, Chiang YR, Chi WC, Kuo YH, Phong AD, Chen CY, Lee TH (2020) Anti-inflammatory effects of peptides from a marine algicolous fungus *acromonium* sp. NTU492 in BV-2 microglial cells. *J Food Drug Anal* 28:89–97
- Hsieh MH, Hsiao G, Chang CH, Yang YL, Ju YM, Kuo YH, Lee TH (2021) Polyketides with anti-neuroinflammatory activity from *Theissenia Cinerea*. *J Nat Prod* 84:1898–1903
- Kaul S, Gupta S, Ahmed M, Dhar KM (2012) Endophytic fungi from medicinal plants a treasure hunt for bioactive metabolites. *Phytochem Rev* 11:487–505
- Kumar VS, Kumaresan S, Tamizh MM, Islam MH, Thirugnanasambantham K (2019) Anticancer potential of NF-kappa B targeting apoptotic molecule flavipin isolated from endophytic *Chaetomium globosum*. *Phytomedicine* 61:152830
- Lee MS, Wang SW, Wang GJ, Pang KL, Lee CK, Kuo YH, Cha HJ, Lin RK, Lee TH (2016) Angiogenesis inhibitors and anti-inflammatory agents from *Phoma* sp. NT0U4195. *J Nat Prod* 79:2983–2990
- Lin FL, Ho JD, Cheng YW, Chiou YCG, Yen JL, Chang HM, Lee TH, Hsiao G (2018) Theissenolactone C exhibited Ocular Protection of Endotoxin-Induced Uveitis by attenuating ocular inflammatory responses and glial activation. 9:326
- Mishra S, Priyanka, Sharma S (2022) Metabolomic insights into endophyte-derived bioactive compounds. *Front Microbiol* 13:835931
- Nakazawa T, Ishiuchi K, Sato M, Tsunematsu Y, Sugimoto S, Gotanda Y, Noguchi H, Hotta K, Watanabe K (2013) Targeted disruption of transcriptional regulators in *Chaetomium Globosum* activates biosynthetic pathways and reveals transcriptional regulator-like behavior of aureonitol. *J Am Chem Soc* 135:13446–13455
- Qi JZ, Wang DC, Yin X, Zhang Q, Gao JM (2020) New Metabolite with Inhibitory Activity against alpha-glucosidase and alpha-amylase from endophytic *Chaetomium globosum*. *Nat Prod Commun* 15:1–9
- Song CG, Ding G, Wu G, Yang J, Zhang MZ, Wang HY, Wei DS, Qin JC, Guo LP (2020) Identification of a Unique Azaphilone produced by *Chaetomium Globosum* isolated from *Polygonatum Sibiricum*. *Chem Biodivers* 17:e1900744
- Tiwari P, Srivastava Y, Bae H (2022) Trends of pharmaceutical design of endophytes as anti-infective. *Curr Top Med Chem* 21:1572–1586
- Wang MH, Jiang T, Ding G, Niu SB, Wang XW, Yu M, Gu YC, Zhang QB, Chen JH, Jia HM, Zou ZM (2017) Molecular epigenetic approach activates silent gene cluster producing dimeric bis-spiro-azaphilones in *Chaetomium Globosum* CBS148.51. *J Antibiot* 70:801–804
- Wang DC, Zhang YM, Li X, Pan HY, Chang MY, Zheng TY, Sun JZ, Qiu DR, Zhang MZ, Wei DS, Qin JC (2017a) Potential allelopathic azaphilones produced by the endophytic *Chaetomium globosum* TY1 inhabited in *Ginkgo biloba* using the one strain-many compounds method. *Nat Pro Res* 31:724–728
- Wen J, Okyere SK, Wang S, Wang JC, Xie L, Ran YA, Hu YC (2022) Endophytic Fungi an effective alternative source of Plant-Derived Bioactive compounds for Pharmacological studies. *J Fungi* 8:205
- Wu HC, Chen YC, Hsieh G, Wang SW, Cheng MJ, Chao CY, Lee TH, Kuo YH (2022) Chemical constituents and their anti-neuroinflammatory activities from the bark of Taiwan incense cedar, *Calocedrus Formosana*. *Phytochemistry* 204:113347
- Yamada Y, Doi M, Shigetani H, Muroga Y, Hosoe S, Numata A, Tanaka R (2008) Absolute stereostructures of cytotoxic metabolites, chaetomugilins A–C, produced by a *Chaetomium* species separated from a marine fish. *Tetrahedron Lett* 49:4192–4195
- Yang MH, Gu ML, Han C, Guo XJ, Yin GP, Yu P, Kong LY (2018) Aureochaeglobosins A–C, three [4 + 2] adducts of chaetoglobosin and aureonitol derivatives from *Chaetomium Globosum*. *Org Lett* 20:3345–3348
- Yang CY, Chen C, Lin CY, Chen YH, Lin CY, Chi CW, Chen YJ, Liu SC, Chang TK, Tang CH, Lai YW, Tsai HJ, Chen JJ, Wang SW (2019) Garcimultiflorone K inhibits angiogenesis through Akt/eNOS- and mTOR-dependent pathways in human endothelial progenitor cells. *Phytomedicine* 64:152911
- Yang MY, Wang YX, Chang QH, Li LF, Liu YF, Cao F (2021) Cytochalasins and azaphilones suitable chemotaxonomic markers for the *Chaetomium* species. *Appl Microb Biotechnol* 105:8139–8155
- Zhang G, Zhang Y, Qin J, Qu X, Liu J, Li X, Pan H (2019) Antifungal metabolites produced by *Chaetomium Globosum* No.04, an endophytic fungus isolated from *Ginkgo biloba*. *Indian J Microbiol* 53:175–180
- Zhang XY, Tan XM, Yu M, Yang J, Sun BD, Qin JC, Guo LP, Ding G (2021) Bioactive metabolites from the desert plant-associated endophytic fungus *Chaetomium Globosum* (Chaetomiaceae). *Phytochemistry* 185:112701

Publisher's Note

Springer Nature remains neutral with regard to jurisdictional claims in published maps and institutional affiliations.